

Towards Quorum Sensing Based Distributed Control for Networks of Mobile Sensors

Brian Geuther¹, Bahareh Behkam²

Abstract—Control and communication for a distributed network of robotic agents is a difficult problem to solve at the microscale. In nature, bacteria utilize chemical signaling to execute controlled movement, communication, and collaborative task completion. Chemotactic response (i.e. biased random walk of bacteria towards a chemo-attractant source) enables effective sensing and creates a biased distribution of bacteria in a field. Quorum sensing allows a robust collective response to be achieved at specific bacteria number densities. In this work, we present a computational model for bio-inspired sensing, communication, and control that is based on the combination of chemotaxis and quorum sensing. We have computationally demonstrated that these bio-inspired strategies can be implemented in synthetic mobile sensor network. Robustness and response time of such systems are also examined.

I. INTRODUCTION

Biologically inspired technology is becoming more prevalent in research. Two significantly important methods of biological distributed organization include chemotaxis and quorum sensing. Chemotaxis is a biological process in which organisms sense and respond to concentration gradients of select chemicals from the environment in order to achieve a directed movement. The directed movement can either be towards a chemo-attractant, a favorable chemical, or away from a chemorepellant. Quorum sensing is a biological process used to control specific functionality based on the measured number density of agents in the system. The process involves releasing and sensing of signaling molecules, called autoinducers, in a field and activating functionality when a specific threshold is sensed. The combination of chemotaxis and quorum sensing can be seen as a method of aggregating agents and then activating functionality. This combination poses advantages in collective microrobotic behavior (e.g. network of mobile sensors) due to the simplicity of the agent's functionality.

Achieving communication of information at microscale contains many limitations. Detecting chemicals within a microscale field is an important task for networked sensors. Currently, fluorescent signals are utilized to provide feedback for specific chemicals detected in a field [1]. This method can produce many false positives or low quality responses. Efforts have been made to improve response, but limitations still exist with providing practical applications [2]. Mobile agents allow for more complex problems to be solved. Magnetic control of microscale agents enables precise control

at this scale but limits the ability for multiple agents to be controlled independently [3]–[6].

In the work presented here, we demonstrate that collaboration between a distributed network of mobile sensors comprise of 100s or even 1000s of agents through the use of chemotaxis and quorum sensing can provide a robust solution to microscale networked sensing. We have developed a computational model that describes the motility, chemotaxis, and quorum sensing of the agents within the system. The movement of individual agents described through a random walk algorithm. The chemotactic behavior model dictates both how a chemical gradient is sensed and what modifications are done to the movement to introduce a bias in the random walk. Quorum sensing behavior model describes the methods used in achieving multi-agent communication. The rest of this paper is organized as follows. In section II, the theoretical basis of the computational model is presented. In section III, the computational model is validated using previously published experimental data. In section IV, chemotaxis and quorum sensing based strategies for distributed control of synthetic microrobotic systems are developed and discussed.

II. MODELING

The objective of this computational model is to provide a platform for simulation and testing of a large population of mobile agents interacting in a field through passive communication. Development of this computational model is described as three submodels including motility, chemotaxis, and quorum sensing behavior.

A. Motility

The motility of flagellated bacteria can be modeled with run and tumble phases. These two phases are distinguished when the bacteria moves in a single direction (run) and re-orientates itself (tumble) as separate actions. Random run and tumble behavior of bacteria, which leads to a random walk, is best modeled as Poisson processes. The exponential distribution can be described as follows:

$$f(t, \lambda_i) = \lambda_i e^{-\lambda_i t} \quad (1)$$

where λ_i is the mean value of the exponential distribution. Experimental observations provide the means for these processes. After a given phase of run or tumble comes to an end, a new timer is generated based on the exponential distribution to be allocated for the agent's next action. The two important factors to keep track for each individual agent are the absolute position and directional bearing. During the run phase, the position of the agent is modified by a constant

¹Department of Mechanical Engineering Virginia Tech, Blacksburg, VA 24061, USA

²Department of Mechanical Engineering and School of Biomedical Engineering and Sciences, Virginia Tech, Blacksburg, VA 24061, USA
behkam@vt.edu

movement rate in the direction of the bearing. Whereas, the tumble phase modifies the bearing. A well-known model organism for flagellated movement is *Escherichia coli* (*E. coli*). Specific to this organism, the movement means under isotropic conditions are $\lambda_{run} = 0.9s$ and $\lambda_{tumble} = 0.1s$ [7]. When a chemical gradient is sensed, these values are modified.

B. Chemotaxis

When a chemo-effector gradient is introduced into the field, *E. coli* exhibit a biased in the random walk. This bias is created through modification of the mean value for run times [7]. The ability to detect a chemical gradient is limited by the biological resolution of sensing a chemical, which is 3 nM for *E. coli* [8]. If a difference between two measured values is greater than this threshold, the agent will exhibit the biased movement. Specifically, the mean run time increases. This provides longer run phases in the direction towards the chemo-attractant with a less likelihood of rotating. Due to the stochastic nature of this movement, an expected bias in the movement can be detected within 10 minutes. This form of movement provides a robust solution in finding both local and absolute maxima within a gradient field searched.

C. Quorum Sensing Behavior

Quorum sensing (QS) is the ability for individual agents within a population to detect when a specific number density of the individuals has been reached. The biological implementation of this behavior is to create, release, and sense signaling molecules in the surrounding environment. When a specific threshold of these molecules has been sensed, certain genetic functionalities are either expressed or suppressed. The model organism selected for this functionality is *Vibrio fischeri* (*V. fischeri*), an abundantly studied model organism for quorum sensing. These bacteria use quorum sensing to express bioluminescence when a high cell density is detected. The specific genetic functionality includes a positive feedback loop for the generation of quorum sensing molecules with a secondary threshold for bioluminescence, as shown in Figure 1 [9].

The purpose of the positive feedback loop in production rate is to encourage all agents in the nearby field to activate their quorum sensing functionality simultaneously. An instantaneous switch to increased production is difficult to achieve in nature. A hill function best models the biological generation rate of the signaling molecules, as shown in equation 2:

$$A_t = (A_1 + A_2 \frac{Q^n}{Q^n + Q_0^n}) \quad (2)$$

where A_t is total generation rate, A_1 is a constant generation rate, A_2 is an increased generation rate, n is the hill coefficient, Q is the measured concentration, and Q_0 is the threshold concentration at which production significantly increases. The hill coefficient controls the slope of the positive feedback loop and in turn the sensitivity for a response to increasing concentration values. A coefficient of 2.5 is used for this

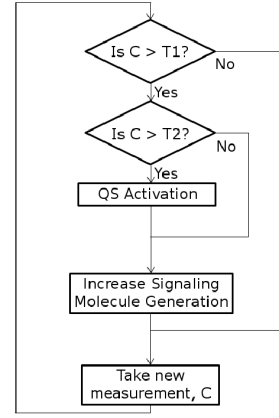


Fig. 1: Quorum sensing control feedback loop where the production of signaling molecules increases after the first threshold (T1) is reached and an additional function such as production of green fluorescent protein (GFP) is executed after a second threshold (T2) is reached.

simulation to adequately match the production rates in *V. fischeri* [9]. Synthetic biology methods can be used to devise synthetic quorum sensing plasmids (with different outputs such as change in motility or green fluorescent protein (GFP) expression) that can be inserted in other bacteria such as *e. coli* to impart them with quorum sensing functionality.

As the signaling molecules are produced, the spatiotemporally varying concentration values must be added to the field. The signaling molecule concentration field is stored in a mesh grid of values. The 2-dimensional average concentration over each grid element is represented by a value at the center of that element, as shown in Figure 2. An agent that interacts with the field does not necessarily have to follow the grid element. As each agent moves, it interrogates the mesh grid to obtain the signaling molecule concentration at its locations. Unless an agent happens to be at the center of an element, an interpolation function is used to calculate the concentration using values from four neighboring elements. Similarly, when an agent releases signaling molecules into the field, the total number of signaling molecules are divided into the the four closest mesh elements.

Upon release from the agents, distribution of the signaling molecules is determined by their diffusion, advection, and degradation. Diffusion and advection cause the molecules to redistribute over time, as described through the mass transport equation:

$$\frac{\partial C}{\partial t} + u_i \frac{\partial C}{\partial x_i} = D \frac{\partial^2 C}{\partial x_i^2} \quad (3)$$

where C is the concentration, u_i is the velocity field, and D is the diffusion coefficient. Degradation of the signaling molecules occurs at a constant rate, as shown in Table I.

Due to the computational power required to solve equation 3, a numerical method known as Alternating Direction Implicit (ADI) is used. This method provides a solution that

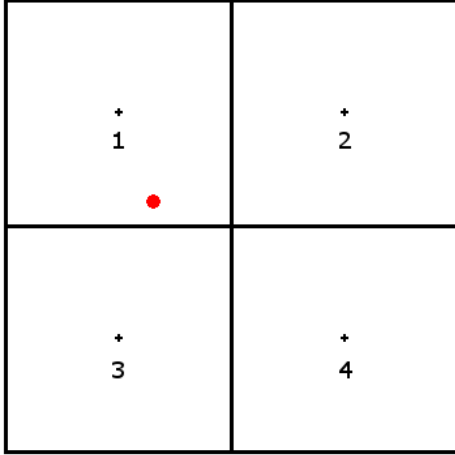


Fig. 2: Representative image of the mesh grid used in quorum sensing. The four black boxes represent four neighboring elements while the red dot represents a simulated agent within the field.

can be computed on a linear time order related to the number of elements within the mesh. The selection of the mesh size is important to allow for reasonable computation time as well as maintaining stability of the results. Equation 3 is solved numerically to determine the new concentration values dependant upon diffusion in a given time step.

D. Model Parameters

There are many variables within this simulation. Where appropriate, biological values were utilized in an attempt to best model an existing system for functionality as well as for computational model validation purposes. A full layout of variables used can be seen in table I. The objective of this numerical model is to present a computational framework for design and/or prediction of population response to an external stimuli, and not be limited to the modeling of existing biological systems.

III. VALIDATION OF THE COMPUTATIONAL MODEL

The objective of this computational model is to simulate a cooperative system that is inspired by nature. This section presents a comparison between the simulation and experimental results as seen in the literature.

A. Chemotaxis Validation

The objective of chemotaxis is to provide a bias random walk based on stochastic movement. The chemotactic response of a population of *E. coli* bacteria is experimentally measured by calculation of the chemotactic partition coefficient (CPC). The CPC method divides the field into multiple partitions and counts the number of observed bacteria. Only two partitions were used for this analysis. Due to the nature of this simulation, knowing the exact positions of each agent, the calculation of the coefficient takes a discrete form shown in equation 4:

TABLE I:
Parameters used in the simulations. Individual values can be readily changed to simulate different environments and synthetic systems.

Variable	Value	Description	Unit
λ_r	0.9 [7]	Average run time	<i>s</i>
λ'_r	1.3 [7]	Chemotactic run time average	<i>s</i>
λ_t	0.1 [7]	Average tumble time	<i>s</i>
λ'_t	0.1 [7]	Chemotactic tumble time average	<i>s</i>
v	20 [7]	Average speed of bacteria	$\frac{\mu m}{s}$
θ	5.93 [7]	Tumble rate	$\frac{rad}{s}$
t_s	0.01	Time step	<i>s</i>
X_f	5000	Field maximum size	μm
X_m	1000	Mesh maximum size	<i>elements</i>
A_1	0.552 [10]	Constant QS signaling molecule generation	$\frac{molecules}{s}$
A_2	5.52 [10]	Upregulated QS signaling molecule generation	$\frac{molecules}{s}$
d	10.8 [10]	Abiotic degradation of QS signaling molecule	$\frac{Percent}{hr}$
Q_0	1.00 [11]	Upregulation value for QS	$\frac{molecules}{\mu m^3}$
Q_t	15.05 [10]	Threshold for QS validation	$\frac{molecules}{\mu m^3}$
C_t	3×10^{-9} [8]	Chemotactic threshold	<i>M</i>
C_g	1×10^{-5} [12]	Chemotactic gradient	$\frac{M}{mm}$
C_g	6.67×10^{-9} [13]	Diffusion of QS signaling molecules	$\frac{m^2}{day}$

$$CPC = \frac{1}{N} \left(\sum_{i=1}^N \left(x_i > \frac{w}{2} \right) - \sum_{i=1}^N \left(x_i < \frac{w}{2} \right) \right) \quad (4)$$

where N is the number of agents, x_i is the position of an agent, and w is the width of the field. Obtaining a positive CPC value infers the agents followed the gradient (positive chemotaxis or movement towards the source of a chemo-attractant). The CPC value can range between -1 and 1, inferring complete repulsion and complete attraction.

The simulation setup for validating the chemotactic behavior is to start all agents at exactly the center of the field. A linear chemical gradient is established along the horizontal axis and agents perform a random walk as described earlier in the paper. Additionally, a second control field is executed with no gradient introduced. As shown in Figure 3, a biased distribution can be seen within the chemotactic field. For 50,000 bacteria after 10 minutes of simulated time, the resulting CPC value is 0.1197. The resulting distribution can be seen in Figure 3. The control presented a CPC value of 0.0040. CPC values in this range match experimental results for a $1 \times 10^{-5} \frac{M}{mm}$ gradient [12].

B. Quorum Sensing Validation

In effort to validate the quorum sensing functionality, biological constants were used to check the steady state response observed in literature. In effort to simulate the isotropic nature of the experimental data collected from bulk samples of bacteria, agents are immobile and randomly

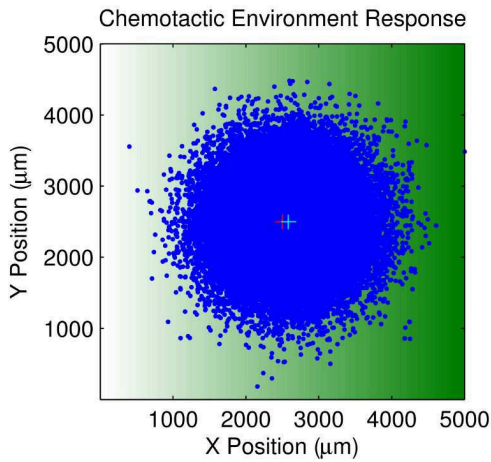


Fig. 3: Positions of agents after 10 minutes of random walking. The starting position for every agent was at the red crosshair at $(2500 \mu\text{m}, 2500 \mu\text{m})$. The resulting average position shifted to $(2419 \mu\text{m}, 2500 \mu\text{m})$, as shown with the cyan crosshair. The average position further shifts to the right with time. The linear chemical gradient is shown with a green background. Intensity of the green color represents the concentration of the chemical.

placed across the entire field. The biological system is expected to have a time-varying response with a strong relation to the number of agents in the field. As shown in Figure 4, for any given time period, the higher number of agents maintain a larger percentage of agents with activated quorum sensing functionality.

It is important to note that although each of the simulations are approaching 100% quorum sensing activation, the absolute concentration of quorum sensing molecules in the field approaches a different steady state value. This steady state value can be used as a modified quorum sensing threshold which will cause different detected densities of agents within a distributed system to activate.

IV. ROBUST RESPONSE OF THE NETWORKED SENSORS

The objective of this analysis is to demonstrate the feasibility of a quorum sensing based strategy for distributed control of microrobotic systems. For the application of distributed mobile sensor networks, there are many important factors to take into account. Here, we focus on using our computational model to determine the quorum sensing threshold required to achieve a desired response of the system. Fine tuning with a known number of agents acting in the system can be effectively used to remove the possibility of achieving false positives within the response. For this simulation, a total of 2500 agents were used within a linear chemo-attractant gradient along the x-axis. The desired response is for a high concentration of agents to aggregate at the chemo-attractant source and activate quorum sensing to display the detection of the source. Agents individually produce signaling molecules that are distributed dynamically within the field as time progresses.

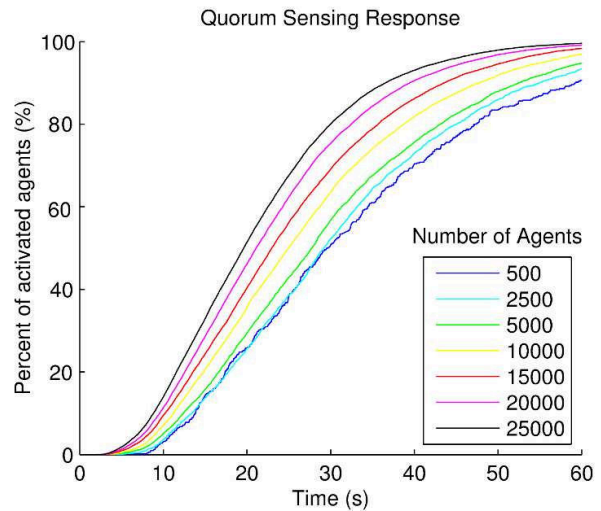


Fig. 4: Normalized quorum sensing response as a function of time. A constant field size is used and a varying number of agents are present in the field. As the number of agents increases, the response time of the system decreases.

With the field size of $5000 \mu\text{m}$, a uniform distribution of 2500 agents will provide a quorum sensing molecule concentration on the order of $14 \frac{\text{molecules}}{\mu\text{m}^3}$ after 1 hour. Due to the desire to detect a source within the field, an expected unequal distribution will cause the number density of agents in certain areas to increase. By raising the threshold from the measured concentration of immobile agents to a larger value, a desired response of the system can be achieved. The higher threshold value used for this study is $15 \frac{\text{molecules}}{\mu\text{m}^3}$. As shown in Figure 5 after an hour of simulated time, the distributed network of sensors has successfully detected the source of the chemo-attractant. Additionally, a false positive region has been detected on the left half of the x-axis at the coordinate $(1000 \mu\text{m}, 2000 \mu\text{m})$.

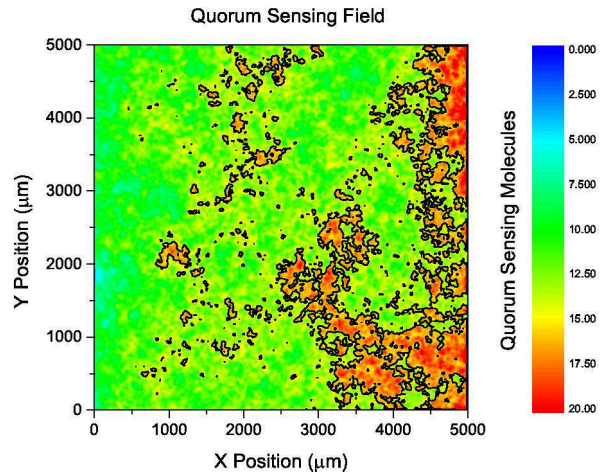


Fig. 5: The signaling molecule distribution within the field after 1 hour of simulated time. The black line provides a boundary for the detection area of $15 \frac{\text{molecules}}{\mu\text{m}^3}$ or greater.

If the threshold value is increased further, the response can be limited to even larger densities. As shown in Figure 6, an increased quorum sensing threshold of $16.5 \frac{\text{molecules}}{\mu\text{m}^3}$ was applied to achieve a more robust response in which there are less substantial false positives detected.

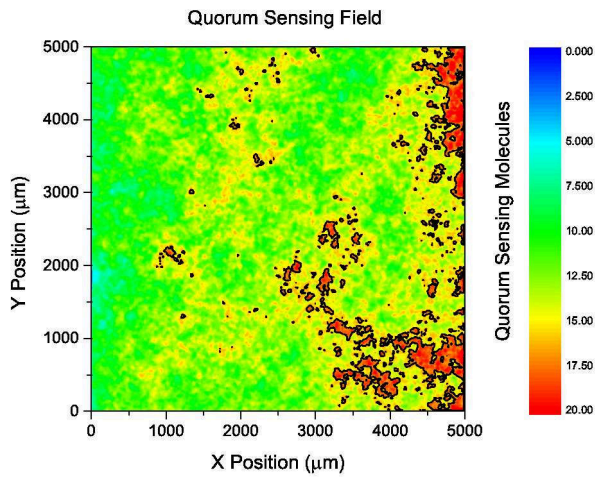


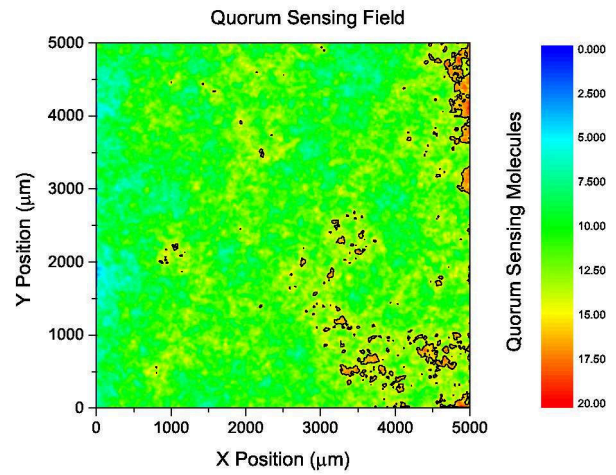
Fig. 6: The quorum sensing molecule distribution within the field after 1 hour of simulated time. The black line provides a boundary for the detection area of $16.5 \frac{\text{molecules}}{\mu\text{m}^3}$ or greater.

Depending upon the desired objectives for the distributed control, various thresholds can be applied to control the response within the system. However, with greater robustness to false positives comes at a trade-off of time required for the response. As shown in Figure 7, the larger threshold of $16.5 \frac{\text{molecules}}{\mu\text{m}^3}$ has not detected the chemo-attractant source at a time of 50 minutes when the two simulations are compared.

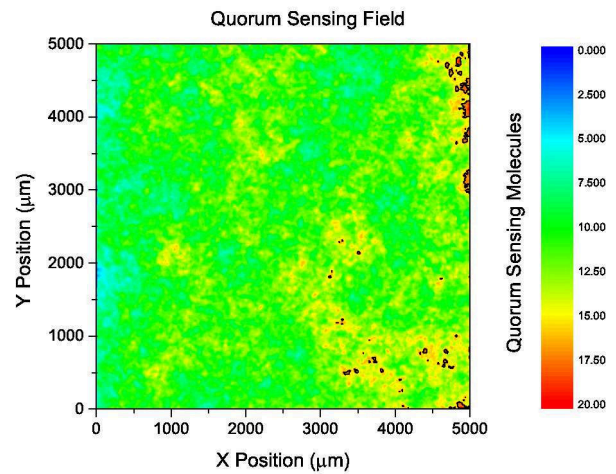
There are many parameters that can be changed within this stochastic control system to alter the behavior. The modification of the quorum sensing threshold with respect to a steady state density threshold can achieve a desired outcome within a field. Larger thresholds reduce the identification of false positives and increase the response time while smaller thresholds increase the chance of false positives and reduce the response time of the quorum sensing network. These values do not change the response time of the chemotactic movement, which must be established to trigger quorum sensing.

V. CONCLUSIONS

In conclusion, bioinspiration in sensing and control can be utilized to aid in the development of robust mobile sensor networks. The application of stochastic movement in the form of biased random walk can allow for searching gradient fields and identifying signaling sources. Additionally, passive communication in the form of quorum sensing can be used to collaborate between many agents within the field. By fine-tuning the specific parameters of this system, a desired response can be obtained. As shown in the results, a trade-off between response time and chance of false positives must be made.



(a)



(b)

Fig. 7: A comparison between the quorum sensing molecule thresholds at 50 minutes of simulated time. (a) has a threshold applied at $15 \frac{\text{molecules}}{\mu\text{m}^3}$ and (b) has a threshold applied at $16.5 \frac{\text{molecules}}{\mu\text{m}^3}$.

VI. FUTURE WORK

The main objective of this work is to develop a simulation environment for the creation and analysis of synthetic stochastic control circuits based on chemotactic and quorum sensing behavior. A chemotactic behavior can be extended to include all methods for modification of movement behavior based on environmental signaling. Quorum sensing functionality can be modified in sensitivity as well as the form of output. Future studies include the modification of additional parameters in chemotactic behavior and quorum sensing functionality in effort to provide low cost solutions for collective robotic systems. Additional fine tuning of the quorum sensing parameters such as the modification of the upregulation value can provide solutions for optimal response time with negligible chance for false positives.

Acknowledgements

The authors would like to thank their colleagues in the MicroN BASE laboratory for simulation discussions. Our special gratitude goes to Mahama Traoré for discussions involving the modeling of chemotactic behavior as well as Ali Sahari and Professor Birgit Scharf (Biological Sciences) for discussion involving quorum sensing modeling. This project was partially supported by the National Science Foundation (IIS-117519).

REFERENCES

- [1] D. Altschuh, S. Oncul, and A. Demchenko, "Fluorescence sensing of intermolecular interactions and development of direct molecular biosensors," *Journal of Molecular Recognition*, vol. 19, no. November, pp. 459–477, 2006.
- [2] A. P. Demchenko, "The problem of self-calibration of fluorescence signal in microscale sensor systems," *Lab on a chip*, vol. 5, no. 11, pp. 1210–23, Nov. 2005.
- [3] L. Arcese, M. Fruchard, and A. Ferreira, "Nonlinear modeling and robust controller-observer for a magnetic microrobot in a fluidic environment using MRI gradients," *2009 IEEE/RSJ International Conference on Intelligent Robots and Systems*, pp. 534–539, Oct. 2009.
- [4] S. Tottori, L. Zhang, F. Qiu, K. K. Krawczyk, A. Franco-Obregón, and B. J. Nelson, "Magnetic helical micromachines: fabrication, controlled swimming, and cargo transport," *Advanced materials (Deerfield Beach, Fla.)*, vol. 24, no. 6, pp. 811–6, Feb. 2012.
- [5] S. Floyd, C. Pawashe, and M. Sitti, "Microparticle manipulation using multiple untethered magnetic micro-robots on an electrostatic surface," *2009 IEEE/RSJ International Conference on Intelligent Robots and Systems*, pp. 528–533, Oct. 2009.
- [6] J.-B. Mathieu, G. Beaudoin, and S. Martel, "Method of propulsion of a ferromagnetic core in the cardiovascular system through magnetic gradients generated by an MRI system," *IEEE transactions on bio-medical engineering*, vol. 53, no. 2, pp. 292–9, Feb. 2006.
- [7] H. Berg and D. Brown, "Chemotaxis in *Escherichia coli* analysed by three-dimensional tracking," *Nature*, vol. 239, pp. 500–504, 1972.
- [8] H. Mao, P. S. Cremer, and M. D. Manson, "A sensitive, versatile microfluidic assay for bacterial chemotaxis," *Proceedings of the National Academy of Sciences of the United States of America*, vol. 100, no. 9, pp. 5449–54, Apr. 2003.
- [9] J. Williams and X. Cui, "Robust and sensitive control of a quorum-sensing circuit by two interlocked feedback loops," *Molecular systems biology*, vol. 4, no. 234, pp. 1–11, 2008.
- [10] A. Pai and L. You, "Optimal tuning of bacterial sensing potential," *Molecular systems biology*, vol. 5, no. 286, p. 286, Jan. 2009.
- [11] J. W. Williams, X. Cui, A. Levchenko, and A. M. Stevens, "Robust and sensitive control of a quorum-sensing circuit by two interlocked feedback loops," *Molecular systems biology*, vol. 4, no. 234, p. 234, Jan. 2008.
- [12] M. A. Traore and B. Behkam, "A peg-da microfluidic device for chemotaxis studies," *Journal of Micromechanics and Microengineering*, vol. 23, no. 8, p. 085014, 2013.
- [13] M. R. Frederick, C. Kuttler, B. a. Hense, and H. J. Eberl, "A mathematical model of quorum sensing regulated EPS production in biofilm communities," *Theoretical biology & medical modelling*, vol. 8, no. 1, p. 8, Jan. 2011.